PARP1 blockade is synthetically lethal in XRCC1 deficient sporadic epithelial ovarian cancers

Reem Ali[1*], Muslim Alabdullah [1, 2*], Adel Alblihy[1], Islam Miligy[2], Katia A. Mesquita[1], Stephen YT Chan[3], Paul Moseley[3], Emad A Rakha[2] and Srinivasan Madhusudan[1,3]**

[1] Translational Oncology, Division of Cancer and Stem Cells, School of Medicine, University of Nottingham, Nottingham University Hospitals, Nottingham NG5 1PB, UK.

[2] Department of Pathology, Division of Cancer and Stem Cells, School of Medicine, University of Nottingham, Nottingham NG51PB, UK.

[3] Department of Oncology, Nottingham University Hospitals, City Hospital Campus, Nottingham NG5 1PB, UK.

[*] = Both equally contributed to the work

Running title: XRCC1 and PARPi synthetic lethality in ovarian cancers

Declarations of interest: none

Word count: 3305

Figure: Six

Abbreviations:

XRCC1: X-ray repair cross- complementing gene 1; PARP1: poly(ADP-ribose) polymerase 1; BER: base excision repair; SSBR: single strand break repair; SSB: single strand break; DSB: double strand break repair; Lig III: Ligase III; PAR: poly (ADP-ribose); PARG: PAR glycohydrolase; KO: knock-out; TMA: tissue microarray; IHC: immunohistochemistry

*** Corresponding author:**

Professor Srinivasan Madhusudan

Translational Oncology, Division of Cancer and Stem Cells, School of Medicine, University of Nottingham, Nottingham University Hospitals, Nottingham NG51PB, UK. Telephone: +44(0)115 823 1850, Fax: +44(0)115 823 1849,

E-Mail: srinivasan.madhusudan@nottingham.ac.uk

ABSTRACT

PARP1 inhibitor (Niraparib, Olaparib, Rucaparib) maintenance therapy improves progression-free survival in platinum sensitive sporadic epithelial ovarian cancers. However, biomarkers of response to PARPi therapy is yet to be clearly defined. XRCC1, a scaffolding protein, interacts with PARP1 during BER and SSBR. In a large clinical cohort of 525 sporadic ovarian cancers, high XRCC1 or high PARP1 protein levels was not only associated with aggressive phenotypes but was also significantly linked with poor progression-free survival ($p = 0.048$ & $p=0.001$ respectively) and poor ovarian cancer-specific survival ($p = 0.020$ & $p=0.008$ respectively). Pre-clinically, Olaparib and Talazoparib therapy were selectively toxic in XRCC1 deficient or knock-out platinum sensitive ovarian cancer cells in 2D and 3D models. Increased sensitivity was associated with DNA double-strand break accumulation, cell cycle arrest and apoptotic cell accumulation. We conclude that XRCC1 deficiency predicts sensitivity to PARP inhibitor therapy. PARP1 targeting is a promising new approach in XRCC1 deficient ovarian cancers.

Key words: Ovarian cancer; XRCC1;PARP; synthetic lethality.

1. INTRODUCTION

The overall survival for patients with advanced ovarian cancer remains poor despite adavances in platinum based chemotherapy. The cytotoxicity of platinum drugs (carboplatin, cisplatin) is directly related to induction of intra-strand and inter-strand DNA adducts in cells. If unrepaired these DNA damaging lesions can promote the development of DNA double strand breaks (DSBs) during replication. Platinum induced DNA damage is detected and processed through the DNA repair mechanisms. Development of personalized therapy strategy targeting DNA repair is an exciting new strategy in ovarian cancer [1]. The enzyme Poly-(ADP)-ribose polymerase 1 (PARP1) is critically involved in DNA repair. PARP1 binds to DNA repair intermediates such as single-strand breaks and gets activated which in turn leads to the synthesis of PAR (poly-ADP-ribose) polymers. PARP1 auto-PARylation recruits other DNA repair factors (including XRCC1) at sites of DNA damage resulting in efficient DNA repair [1]. BRCA1 and BRCA2 are critical genes involved in the repair of double strand breaks (DSB) through homologous recombination (HR). Women carrying deleterious germline mutations in the BRCA1 or BRCA2 genes have a high risk of developing ovarian cancers [2]. Synthetic lethality exploits inter-gene relationships where the loss of function of either of two related genes is non-lethal, but loss of both causes cell death. This offers the potential to specifically target cancer cells through inhibition of a gene known to be in a synthetic lethal relationship with a mutated tumour suppressor gene. Synthetic lethality approach using PARP inhibitors is an exiciting new strategy in BRCA deficient ovarian cancers. PARP inhibitors block PARP1 catalytic activity therby preventing auto-PARylation. As a result, base excision repair (BER) recruitment is impaired, PARP1 binding to DNA intermediate is stabilised which disrupts replication fork progression leading onto DSB accumulation and apoptosis [1]. In BRCA germline deficient or platinum sensitive ovarian

cancers, PARP1 inhibitor (Niraparib, Olaparib, Rucaparib) maintenance therapy was recently shown to substantially improve progression-free survival in ovarian cancer patients [3-6]. However, not all patients respond to PARP inhibitor therapy; either due to intrinsic or acqwquired resistance to PARP inhibitors [1, 7]. Therefore the development of alternative synthetic lethality targets is urgently needed in epithelial ovarian cancers.

XRCC1 (X-ray repair cross- complementing gene 1) is a scaffolding protein with essential roles in DNA repair. The N-terminal domain of XRCC1 binds to DNA strand breaks [8, 9]. The central breast cancer gene 1 C-terminal (BRCT I) domain interacts with poly(ADP-ribose) polymerase 1 (PARP1) , and the additional C-terminal BRCT II domain binds to Ligase III (LIG III) . XRCC1-LIGIII heterodimer is a key player in base excision repair (BER) and single strand break repair (SSBR). XRCC1 interacts with PARP1 and also coordinates BER/SSBR. XRCC1 also has roles in alternative non-homologous end joining (alt-NHEJ) pathway for double strand breaks (DSBs). XRCC1 deficiency delays SSB rejoining leading onto SSBs and if unrepaired, eventually to double strand breaks (DSBs) [8, 9]. In addition, XRCC1 deficiency/mutation can also hyper-activate PARP1 [10]. XRCC1 deficiency potentiates chemotherapy cytotoxicity [8] including platinum sensitivity in ovarian cancer cells [11].

We hypothesized that XRCC1 could be a promising alternative synthetic lethality target in ovarian cancers. In the current study we have comprehensively investigated the expression of XRCC1 and PARP1 proteins in a large cohort of 525 human ovarian cancers and have confirmed their association with aggressive phenotypes, platinum sensitivity and survival. Clinically relevant PARP inhibitors Olaparib and Talazoparib were selectively toxic in

XRCC1 deficient ovarian cancer cells. We conclude that XRCC1 deficiency is a predictor of PARP inhibitor sensitivity in ovarian cancers.

2. METHODS

2.1. Clinical study

2.1.1. Patients: Investigation of the expression of XRCC1, PARP1, BRCA1 and BRCA2 proteins was carried out on tissue microarrays of 525 consecutive ovarian epithelial cancer cases treated at Nottingham University Hospitals (NUH) between 1997 and 2010. Patients were comprehensively staged as per the International Federation of Obstetricians and Gynaecologists (FIGO) Staging System for Ovarian Cancer. Overall Survival was calculated from the operation date until the 1st of October 2016 when any remaining survivors were censored. Progression-free survival was calculated from the date of the initial surgery to disease progression or from the date of the initial surgery to the last date known to be progression-free for those censored. Platinum resistance was defined as patients who had progression during first-line platinum chemotherapy or relapse within 6 months after completion of chemotherapy. Patient demographics are summarized in Supplementary Table S1. None of the tumors were BRCA germ-line deficient.

2.1.2. Tissue microarray (TMA) and immunohistochemistry (IHC): TMAs were constructed as described previously (Kononen *et al*, 1998). Briefly, triplicate tissue cores with a diameter of 0.6mm were taken from the tumour and arrayed into a recipient paraffin block using a tissue puncher/arrayer (Beecher Instruments, Silver Spring, MD, USA) as previously described (Kononen *et al*, 1998). Four micron sections of the tissue array block were cut and placed on Surgipath X-tra Adhesive microscope slides (Leica Microsystems) for immunohistochemical staining. Immunohistochemical staining was performed using Novocastra Novolink polymer detection system according to manufacturer instructions (Leica Microsystems, Newcastle, UK). Pre-treatment of TMA sections was performed with citrate buffer (pH 6.0, 20 min, Microwave). A set of TMA sections were incubated for 30 min

at room temperature with 1:250 anti-XRCC1 mouse monoclonal antibody (Ab-1, clone 33-2-5, Thermoscientific, Fremont, CA). A set of TMA sections were stained with mouse anti-human PARP1 antibody (clone 46D11, Cell signalling, USA) (1:600) for 60 min incubation in room temperature. A set of TMA sections were stained with anti-BRCA1 (Merck Millipore, UK) (1:200) and further set were stained with anti-BRCA2 (Abcam, UK) (1:100), both were incubated for 1h at room temperature. Sections were counterstained with haematoxylin. Negative controls with no primary antibody were included in each run. Cases with multiple cores were scored and the average was used as the final score.

2.1.3. Evaluation of immune staining: Whole field inspection of the core was scored, and the subcellular localisation of each marker was identified (nuclear, cytoplasm, cell membrane). Intensities of subcellular compartments were each assessed and grouped as follows: 0 = no staining, 1 = weak staining, 2 = moderate staining, 3 = strong staining. The percentage of tumour cells in each category was estimated (0–100%). H-score (range 0–300) was calculated by multiplying the intensity and the percentage of staining. For XRCC1, Low/negative nuclear level was defined by median of H-score of ≤ 100. H score of <80 nuclear PARP1 staining was considered as low/negative which was identified by the median. For BRCA1 nuclear H-score <80 was considered low/negative. While, H-score < 120 were considered low/ negative for nuclear BRCA2 expression. Both BRCA1/BRCA2 cut off points were identified by X-tile. Not all cores within the TMA were suitable for IHC analysis due to missing cores or absence of tumour cells.

2.1.4. Statistical analysis: This was performed using SPSS v 22 (Chicago, IL, USA) for Windows. Association with clinical and pathological parameters using categorised data was examined using Chi-squared test. All tests were 2-tailed. Survival rates were determined using Kaplan–Meier method and compared by the log-rank test. All analyses were conducted using Statistical Package for the Social Sciences (SPSS, version 22, Chicago, IL, USA)

software for windows. P value of less than 0.05 was identified as statistically significant. This work was approved by the Nottingham Research Ethics Committee.

2.2. Pre-clinical study

2.2.1. Compounds and reagents: Olaparib (AZD2281) was kindly provided by AstraZeneca Pharmaceuticals. Talazoparib and PDD00017273 was purchased from (Selleckchem, UK). The antibodies used in the current study are as follows; XRCC1 antibody clone (33-2-5) (Thermofisher, UK), histone H2AX phosphorylated at Ser^{139} (γH2AX; 05–636; Millipore, UK) and PARP1 antibody (Cell signalling, USA). Pre-validated XRCC1 siRNA was purchased from Invitrogen. Lipofecamine3000 reagent, Calcein AM and Ethidium homodimer -1 all were purchased from Thermofisher, UK.

2.2.2. Cell lines and culture: A2780 (platinum sensitive), A2780cis (platinum resistant) and OVCAR3 , OVCAR4, PE04 and SKOV3 cell lines were purchased from American Type Culture Collection (ATCC, Manassas, USA) [12].Cells were cultured in RPMI medium supplemented with 10%FBS and 1% penicillin streptomycin. To maintain cisplatin resistance in A2780cis, cells were exposed to 1μM cisplatin every 2-3 passages.

2.2.3. Targeted next generation sequencing: Genomic DNA was extracted from cell lines using the PicoPure™ DNA Extraction Kit (Thermofisher,UK). Targeted next-generation sequencing was used to identify genomic variants in A2780 and A2780cis. Library preparation and sequencing was conducted by Source Biosciences (Nottingham, UK).

2.2.4. Transient SiRNA transfection: Cells were seeded at 60-70% confluency in t25 flasks overnight, XRCC1 siRNA were delivered to the cells in opti-mem using Lipofecamine 3000 reagent (Invitrogen, UK) as per the manufacturer's protocol. Cell lysates were collected in RIPA buffer (Sigma, UK) supplemented with phosphatase inhibitor cocktail and protease

inhibitors cocktails (Sigma,UK). The efficiency of transfection was confirmed using western blotting.

2.2.5. CRISPR Knock-out of XRCC1: A2780 cells were transfected with oligonucleotides carrying gRNA silencing XRCC1cloned in a Plv-U6g-EPCG plasmid (Sigma, UK).Briefly, cells were seeded at 50- 60 % confluency in 6 well plates overnight. Cells were transfected with 2-3 µg of DNA using Lipofectamine 3000(Invitrogen, UK) in an Opti-MEM medium. After 48 hours Puromycin selection started for stable clones. A2780 cells were selected in 5µg/ml puromycin for 14 days. The efficiency of XRCC1_KO was confirmed using western blot analysis. Multiple clones were selected and used in the current study.

2.2.6. Clonogenic assays: 250 cells were seeded in 6- well plates overnight. Olaparib and talazoparib and PDD00017273 were added at the indicated concentrations. The plates were left in the incubator for 14 days, after incubation colonies were washed with PBS, fixed and stained with crystal violet, acetic acid and methanol mixture and counted.

2.2.7. Cell Proliferation assays: 100 cells /well were seeded in 96-well plates, Left to adhere overnight. Olaparib, talazoparib and PDD00017273 were tested at the indicated concentrations. After 5 days cell viability was measured by cell titer cell proliferation assay (MTS) (Promega, UK).

2.2.8. Cell cycle analysis: Cells were seeded in 6- well plates overnight then treated with 10µM of Olaparib or 5 µM of talazoparib or 10 µM of PDD00017273 for 24 hours. Cells were collected by trypsinization and washed with ice cold PBS, then fixed in 70% ethanol for 30 mins. Ethanol was washed away and the cells were then treated with RNase 5µg/ml and stained with 10ug/ml propidium iodide (Sigma Aldrich).

2.2.9. Detection of DSBs by γH2AX staining: Cells were seeded in 6- well plates overnight then treated with 10µM of Olaparib or 5 µM of talazoparib or 10 µM of PDD00017273 for 24 hours. Cells were collected by trypsinization and washed with ice cold PBS, then fixed in

70% ethanol for 30 mins. Ethanol was washed away and the cells were stained with phospho Histone (γH2AX) Ser139 FITC antibody.

2.2.10. Annexin-V assay for apoptosis: Cells were seeded in 6- well plates overnight then treated with 10μM of Olaparib or 5 μM of Talazoparib 10 μM of PDD00017273 for 24 hours. Cells were collected by trypsinization, washed with ice cold PBS, stained with AnnexinV detection kit (BD biosciences) and analysed by Flow cytometry.

Confocal microscopy: Cells were seeded on the cover slips overnight, then treated with PDP00017273 for the indicated time-points. The cells were fixed with 4% (w/v) paraformaldehyde for 30 min, permeabilized with 0.1% (w/v) Triton X100 (ThermoFisher) for 30 min and blocked with 3% (w/v) BSA for 1 h. Cells were incubated with anti-Poly(ADP-Ribose) polymer antibody (Abcam, ab14459) or with anti- 53BP1 (Cell Signalling, catalogue no. 4937S) and anti γH2AX (Merck millipore clone JBW301) overnight at 4°C. Slides were prepared in duplicates. Imaging was carried out using Leica SP2 confocal laser scanning microscope. For analysis a minimum of 100 cells per slide were counted.

2.2.11. Invasion and migration assays: A2780 (control) and A2780 (XRCC1_KO) were seeded in the Upper chamber of polycarbonate membrane inserts (8 μm pore size), (Cell biolabs,UK) in serum free medium and left to migrate toward 10% serum containing medium for 24 hours. After 24 hours medium containing non- invasive cells were aspirated from the inserts and the inner was washed with distilled water then stained with crystal violet for 10 minutes. Cells were extracted and 100 μL from each sample were transferred to 96-well microtiter plate for measuring OD at 560nm. For migration assays, cells were seeded in 96 well plate containing hydrogel spot non migratory area, left to adhere overnight and then the hydrogel area was digested and cells were left to migrate for 20 hours. Then the wells

were washed three times, fixed and stained as per manufacturer protocol. Cell migration images were analysed by Imagej software.

2.2.12. Generation of 3D spheroids: A2780 control & XRCC1_ KO were seeded in ultra-low attachment 6-well plates using the promo cell tumour spheres medium. After 14 days, cells were treated with the indicated concentrations of Olaparib, Talazoparib or PDD00017273. Then cells were fixed with formaldehyde 3.7% and stained with 2µM calcein AM and 1.5µM ethidium homodimer-1. Imaging was carried out using Leica SP2 confocal laser scanning microscope. Quantification of live/dead staining was carried out by flow cytometry.

2.2.13. Statistical analysis: Statistical data are presented as mean ± SD of at least three independent biological experiments. *P* values were calculated with either the Student two-tailed *t* test and one way ANNOVA for normally distributed datasets or the nonparametric Mann–Whitney two-tailed *U* test.

3. RESULTS

3.1. XRCC1 expression in ovarian cancers: A total of 442 tumours were suitable for analysis of XRCC1 nuclear expression (Figure 1A) as not all cores within the TMA were suitable for IHC analysis due to missing cores or absence of tumour cells. 147/442 (33.3%) tumours were low for XRCC1 expression, and 295/442 (66.7%) of the tumours were high in expression (Supplementary Table S2). High expression was significantly associated with serous cystadenocarcinomas ($p < 0.0001$) and higher FIGO stage at presentation ($p = 0.001$). In addition, tomour with high XRCC1 expression were likely to have measurable disease before chemotherapy ($p = 0.002$) indicating sub-optimal debulking at surgery. Platinum resistance was defined as patients who had progression during first-line platinum chemotherapy or relapse within 6 months after completion of chemotherapy. Patients with tumours with high XRCC1 expression were significantly more likely to be resistant to platinum treatment ($p = 0.003$) (Supplementary Table 2). High XRCC1 expression in tumours showed an adverse clinical outcome with progression-free survival (PFS) ($p = 0.048$) (Figure 1B) and poor ovarian cancer-specific survival (OCSS) ($p = 0.020$) (Figure 1E) compared with tumours that had low XRCC1 expression. Together the data provides clinical evidence that high XRCC1 is a feature of aggressive ovarian cancers and predicts platinum resistance and poor survival in patients.

3.2. PARP1 expression in ovarian cancers: A total of 301 tumours were suitable for analysis of PARP1 nuclear expression (Figure 1A) as not all cores within the TMA were suitable for IHC analysis due to missing cores or absence of tumour cells. 208/401 (51.9%) tumours were high for PARP1 expression and 193/401 (48.1%) of the tumours were low in expression. High expression was significantly associated with serous cystadenocarcinomas

(p <0.00001), higher grade (p = <0.00001), and measurable disease before chemotherapy (p= 0.024) compared with low expression tumours (Supplementary Table 3). High PARP1 expression in tumours showed adverse clinical outcome with poor PFS (p = 0.001) (Figure1C) and poor OCSS (p = 0.008) (Figure1F) compared with tumours that had low PARP1 expression. The data suggests that high PARP1 expression has predictive and prognostic significance in ovarian cancers.

3.3. XRCC1/PARP1 co-expression and ovarian cancers: We then conducted PARP1/XRCC1 co-expression analysis. Tumours with high expression of both PARP1 and XRCC1 showed significant correlation with serous cystadenocarcinoma subtype (p <0.0001), high grade of malignancy (p=0.002) and residual disease before the initiation of chemotherapy (p=0.004) (Supplementary Table S4). Tumours that have low PARP1/XRCC1 protein expression have non-significant improvement in PFS (p=0.090) (Figure 1D) and favourable OCSS (p = 0.010) (Figure 1G).

3.4. Multivariate analysis: In cox multivariate model, platinum sensitivity (p<0.001) and XRCC1 (p=0.016) were independently associated with PFS. For OCSS, platinum sensitivity (p<0.001) and PARP1 (p=0.023) were independently linked with survival (Supplementary Table S5).

Taken together the clinical data provides evidence that XRCC1 deficiency is associated with platinum sensitivity. PARP targeting could be promising approach in XRCC1 deficient ovarian cancers. We proceeded to pre-clinical evaluation in XRCC1 deficient ovarian cancer cell lines.

3.5. XRCC1 deficiency and PARP inhibitor sensitivity in ovarian cancer cells: PARP1 inhibitors (Olaparib, Niraparib and Rucaparib) are standard maintenance therapies to prolong PFS in platinum sensitive sporadic ovarian cancers. Previously, we shown that low XRCC1 level was linked to platinum sensitivity in ovarian cancers [11]. XRCC1 deficient ovarian cancer cell lines were also sensitive to platinum treatment in that study [11]. We therefore tested the hypothesis that PARP inhibitor therapy could be synthetically lethal in XRCC1 deficient ovarian cancer cells.

A2780 is a well described platinum sensitive ovarian cancer cell line established from a patient with previously untreated ovarian cancer and A2780cis is a platinum resistant cell line developed by chronic exposure of the parent cisplatin-sensitive A2780 cell line to increasing concentrations of cisplatin [12]. In targeted deep sequencing we did not identify any mutations in BRCA1 or BRCA2 genes. In clonogenic assay, we first confirmed platinum sensitivity or resistance in A2780 and A2780cis cells respectively (Figure 2A). We then depleted XRCC1 using siRNAs in A2780 and A2780cis cells (Figure 2B). XRCC1 deficiency leads to single strand break (SSB) accumulation which gets converted to double strand breaks (DSBs) in cells. XRCC1 deficiency has previously been shown to activate PARP1[10]. In XRCC1 deficient ovarian cancer cells, we observed increased PARP1 protein levels compared to control cells (Figure 2C). Olaparib (PARP inhibitor) was significantly cytotoxic in XRCC1 deficient A2780 cells compared to control A2780 cells (Figure 2D). Increased cytotoxicity was associated with significant accumulation of γH2AX (Figure 2E), G2M cell cycle arrest (Figure 2F) and increased apoptosis (Figure 2G). In A2780cis XRCC1 deficient cells, although, Olaparib modestly increased γH2AX (Figure 2E), G2M cell cycle arrest (Figure 2F) and increased apoptotic cells (Figure 2G) Olaparib did not significantly increase cytotoxicity as assessed by clonogenic assays (Figure 2D). The data therefore suggests preferential cytotoxicity of Olaparib in XRCC1 deficient platinum sensitive A2780 ovarian cancer cells. To confirm this observation

further we tested a panel of additional ovarian cancer cell lines; OVCAR3, OVCAR4, PEO4 and SKVO3 [12]. XRCC1 depletion in OVCAR3, OVCAR4, PEO4 and SKVO3 cells increased sensitive to Olaparib therapy compared to control cells (Figure 2H, 2I, 2J, 2K).

To validate further, we generated XRCC1 knock-out (KO) in A2780 cell line using CRISPR/cas-9 methodology (Figure 3A). A2780 (XRCC1_KO) cells were similarly sensitive to Olaparib treatment (Figure 3A). We speculated that the increased toxicity observed in XRCC1 deficient cells may be due to not only PARP inhibition but also due to the ability of Olaparib to "trap" PARP proteins thereby leading to SSB and DSB accumulation. To test this hypothesis, we evaluated another clinically relevant PARP inhibitor Talazoparib which is at least 100 times more potent than Olaparib for PARP trapping. As shown in (Figure 3C), XRCC1_KO cells were hypersensitive to Talazoparib therapy. We further confirmed Talazoparib sensitivity in additional ovarian cancer cell lines. XRCC1 depleted OVCAR4, PE04 and SKOV3 cells were extremely sensitive to Talazoparib treatement (Supplementary Figure S2A, S2B, S2C). Olaparib and Talazoparib sensitivity in A2780(XRCC1_KO) cells were associated with increased DNA damage as evident by increased γH2AX nuclear foci (Figure 2D &2E), 53BP1 foci accumulation (Figure 2D& 2F). We further validated DSBs accumulation by γH2AX flow cytometry staining. As expected, Olaparib treatment in A2780 (XRCC1_KO) cells leads to γH2AX accumulation (Figure 4A), G2M cell cycle arrest (Figure 4B) and increased apoptosis (Figure 4C). Talazoparib treatment A2780 (XRCC1_KO) cells was associated with substantial γH2AX accumulation (Figure 4D), G2M cell cycle arrest (Figure 4E) and high levels of apoptosis (Figure 4F).

At sites of DNA damage, PARP1 is recruited where it induces the synthesis of poly (ADP-ribose) (PAR). PARylation of PARP1 and other DNA repair factors is essential for coordination of DNA repair. PARylation is transient and reversible.

PAR glycohydrolase (PARG) is a key factor in the PAR degradation pathway [13-15]. PAR is degraded by PARG through its endo- and exoglycosidase activities. Recently, PARG has emerged as a promising drug target in cancer. The specific PARG inhibitor PDD00017273 was shown to induce synthetic lethality in BRCA1, BRCA2, PALB2, FAM175A (ABRAXAS) and BARD1 deficient breast cancer cells [16, 17]. We therefore tested cellular activity of PDD00017273 in XRCC1 deficient ovarian cancer cells. As shown in Figure 5A, 5B, 5C and 5D, we did not observe any increased sensitivity to PDD00017273 in XRCC1 deficient ovarian cancer cells.

3.6. 3D spheroid studies: To recapitulate *in vivo* system, we generated 3D-spheroids of A2780 control and A2780_ XRCC1 KO cells. Similar to control cells, untreated XRCC1 KO cells retain spheroid forming capacity (Figure 5E). However, upon Olaparib treatment, in XRCC1 KO spheroids, there was not only reduction in spheroid size (Figure 5E) but also accumulation of apoptotic cells (Figure 5G) compared to control spheroids (Figure 5E & 5F). Interestingly, Talazoparib therapy induced a striking reduction in spheroid size (Figure 5E) and viability in XRCC1 KO cells compared to control cells (Figure 5E & 5G). However, PDD00017273 (PARGi) did not affect spheroid size or induce cell death (Figure 5E & 5G). Together, the data provides further evidence that XRCC1 deficient cells are sensitive to PARP inhibitors but not to PARG inhibition in ovarian cancer cells.

Given the potential role for DNA repair in migration and invasion [18, 19], we also tested XRCC1 proficient and XRCC1_KO cells in mgration and invasion assays. As shown in Figure 6A and 6B, compared to control cells, XRCC1_KO_A2780 cells were less migratory and invasive implying a role for XRCC1 in these cellular processes in ovarian cancer cells.

3.7. BRCA and XRCC1 co-expression in ovarian cancers: To evaluate the clinicopathological significance of BRCA1 or BRCA2 protein expression in sporadic ovarian cancers, we completed BRCA1 and BRCA2 staining by immunohistochemistry in the ovarian cancer cohort (Supplementary Figure S2D). We then proceeded to XRCC1/BRCA co-expression analyses. The full data is shown in Figure 6C & 6D, Supplementary Figures S3 & S4 and Supplementary Tables S6, S7, S8 & S9. As shown in supplementary Figure S3, in BRCA1 low expressing tumours, high XRCC1 was associated with poor PFS (borderline non-significant, p=0.061) (Supplementary Figure S3A) and OS (p=0.025) (Supplementary Figure S3B). Similarly, in BRCA2 high tumours, high XRCC1 expression was associated with poor PFS (p=0.003) (Supplementary Figure S3G) and OS (p=0.003) (Supplementary Figure S3H). Additionally, high BRCA2/XRCC1 co-expression was significantly associated with poor PFS (p= 0.016) (Figure 6C) and OS (p= 0.010) (Figure 6D). Similarly, high BRCA1/XRCC1 co-expression remained associated with PFS (p= 0.063) (Supplementary Figure S4A) and OS (P= 0.006) (Supplementary Figure S4B). Together the data suggests that XRCC1 has predictive or prognostic significance in BRCA high or low tumours.

4. DISCUSSION

The scaffolding protein XRCC1 is a key player in BER, SSBR, and alt-NHEJ. XRCC1 deficiency delays SSB rejoining induces mutations and results in elevated levels of sister chromatid exchanges [8, 9]. In addition, XRCC1 deficiency or mutation can also hyper-activate PARP1 [10]. XRCC1 depletion increases ionizing radiation and chemotherapy sensitivity in cells [8, 9]. Genetic polymorphisms in XRCC1 may influence cancer risk and response to platinum based chemotherapy in patients [20-23]. In ovarian cancer patients

XRCC1 Arg399Gln and XRCC1 Arg194Trp polymorphism may influence clinical outcome [22].

In a previous preliminary study of 195 sporadic ovarian cancer patients treated at Nottingham University Hospitals (NUH) between 2000 and 2007, we have shown that XRCC1 overexpression was linked to platinum resistance and poor PFS [11]. We have since expanded this cohort to include a further 330 patients with sporadic ovarian cancer treated from 2007 to 2010. In this large cohort of 525 ovarian tumours, we not only confirmed our previous observation but have also evaluated the expression of PARP1, BRCA1 and BRCA2 proteins. In addition, we have shown that PARP1 overexpression also impacted negatively on PFS and OCSS. The data would concur with previous studies also showing predictive significance of PARP1 in ovarian cancers[24, 25]. As PARP1 and XRCC1 interact with each other during BER [26], we also performed co-expression analyses in ovarian cancer cohorts. We demonstrate that patients with tumours that have low PARP1 and low XRCC1 expression have better PFS and OCSS.

Ovarian cancer patients with germ-line mutations in BRCA1 and BRCA2 have been shown to clinically benefit from PARP inhibitor therapy [3-6]. However, biomarkers of response in sporadic tumours are an area of intense investigation [27]. Homologous recombination repair (HRR) deficiency assays (such as targeted multiplex sequencing, genomic scars, functional assays) and altered DNA repair gene and/or protein expression in tumours are promising approaches to personalize PARP inhibitor therapy in ovarian cancers [27]. Previously we have shown that XRCC1 deficient ovarian cancer cells are sensitive to platinum treatment [11]. A previous synthetic lethality screening study using a large siRNA library identified XRCC1 as a potential synthetic lethality partner for PARP inhibition [28]. In the current

study, we provide confirmatory pre-clinical evidence that XRCC1 deficient ovarian cancer cell lines are hypersensitive to PARP inhibitor therapy through synthetic lethality. A model for synthetic lethality has been suggested previously [29] and summarized as follows; PARP1 binds to sites of single strand breaks. Activation of PARP1 leads to the synthesis of PAR (poly-ADP-ribose) polymers. Auto-PARylation of PARP1 and PARylation of other proteins recruits XRCC1 (and other BER factors) to sites of DNA damage promoting DNA repair. Inhibition of PARP1 catalytic activity (by Olaparib, Talazoparib) prevents auto-PARylation, impairs BER recruitment and stabilises binding of PARP1 to DNA intermediate. DNA-bound immobilised PARP-1 disrupts replication fork progression, leads to double-strand break (DSB) accumulation and DSB-mediated apoptosis. In XRCC1 deficient cells with increased SSB accumulation, PARP inhibition mediated accumulation of DSB is more pronounced compared to XRCC1 proficient cells thereby leading to synthetic lethality. Accordingly in XRCC1 deficient ovarian cancer cells, Olaparib or Talazoparib therapy lead to DSB accumulation, cell cycle arrest and induced apoptosis. Although our data suggests that XRCC1 deficient ovarian cancer cells are more sensitive to Talazoparib compared to Olaparib, it is important to recognise that Talozoparib is a much more potent PARP inhibitor and the concentration of Talozoparib (5μM) is substantially more cytotoxic than the concentration of Olaparib (10 μM) used in our study. Moreover, further *in vivo* studies will also be required to evaluate the clinical potential of this approach in XRCC1 deficient ovarian cancers. In XRCC1 deficient breast cancer models, we have recently confirmed PARP inhibitor sensitivity compared to XRCC1 proficient breast cancer cells [30]. Taken together, the data presented provides strong evidence for a new synthetic lethality strategy in XRCC1 deficient ovarian and breast cancers using PARP inhibitors.

Hoch et al demonstrated that XRCC1 knockdown increased PARP1 activity [10]. An interesting observation in the current study was that we also observed an increase in the expression of PARP1 in XRCC1 deficient cells. In a recent study in breast cancers, we similarly showed that XRCC1 deficient breast cancer cells also have increased PARP1 expression compared to wild type cells [30]. We speculate that increased PARP1 level may also contribute to a hyperactive PARP1 status seen in XRCC1 deficient cells which accumulate single strand breaks. Interestingly, emerging evidence suggests that PARP1 may be subjected to transcriptional regulation such as through Sp-1 transcription factor [31]. Whether such a mechanism operates in XRCC1 deficient cells is unknown but will be an interesting area for future investigation.

In previous studies in melanoma [18] and clear cell renal cancer cells [19], XRCC1 depletion was shown to promote invasion. In addition, we have recently shown that XRCC1 depletion in breast cancer DCIS cells promote invasion [30]. We therefore explored the role of XRCC1 in ovarian cancer cells. Interestingly, XRCC1 depletion resulted in reduction in invasion and migration in A2780 cells. Taken together, the data would imply differential roles of XRCC1 in influencing invasion or migration indifferent tumour types.

A recent study suggested that XRCC1 deficient cells may also be sensitive to PARG inhibitor treatment [32]. PARG inhibition was shown to increase PAR level and deplete of cellular NAD in that study [32]. However, we did not observe increased sensitivity in PARG inhibitor (PDD00017273) treated XRCC1 deficient ovarian cancer cells. The data would imply that PARG inhibitor sensitivity could be cell line dependent. In a recent study by Pillay et al, differential sensitivity to PARG inhibitor (PDD00017273) and PARP inhibitor (Olaparib) was demonstrated in a panel of ovarian cancer cell lines [33]. The authors showed that

PARGi sensitivity in certain ovarian cancer cell lines was due to replication vulnerabilities that render cells dependent of PARG activity for survival. PARG inhibiton in this context induced synthetic lethality [33]. On the other hand, synthetic lethality due to PARP inhibitors is related to impaired DNA repair capcity such due to BRCA deficiency [1] or due to XRCC1 deficiency shown in the current study.

In conclusion, we provide clinical and pre-clinical evidence that XRCC1 deficient ovarian cancers may be suitable for synthetic lethality targeting using PARP inhibitors.

Acknowledgements:

We would like to thank Nottingham Biobank for providing tissue microarrays.

Authors' contributions:

MA: IHC, scoring, data analyses, data interpretation, manuscript preparation, approval of final manuscript.

RA: Tissue culture experiments, gene knock-down/knock-out studies, molecular biology, data analyses, data interpretation, manuscript preparation, approval of final manuscript.

AA: Tissue culture experiments, gene knock-down/knock-out studies, molecular biology, data analyses, data interpretation, manuscript preparation, approval of final manuscript.

IM: IHC, scoring, data analyses, data interpretation, manuscript preparation, approval of final manuscript.

SYT: Data analyses, data interpretation, manuscript preparation, approval of final manuscript.

PM: Data analyses, data interpretation, manuscript preparation, approval of final manuscript.

EAR: Study design, data analyses, data interpretation, manuscript preparation, approval of final manuscript.

SM: Study design, data analyses, data interpretation, manuscript preparation, approval of final manuscript.

Competing interests: The authors have declared that no competing interest exists.

REFERENCES

[1] C.J. Lord, A. Ashworth, PARP inhibitors: Synthetic lethality in the clinic, Science, 355 (2017) 1152-1158.
[2] C.S. Walsh, Two decades beyond BRCA1/2: Homologous recombination, hereditary cancer risk and a target for ovarian cancer therapy, Gynecol Oncol, 137 (2015) 343-350.
[3] M.S.a.D. Edessa, PARP inhibitors as potential therapeutic agents for various cancers: focus on niraparib and its first global approval for maintenance therapy of gynecologic cancers, Gynecol Oncol Res Pract., 4 (2017) 18.
[4] J. Ledermann, P. Harter, C. Gourley, M. Friedlander, I. Vergote, G. Rustin, C. Scott, W. Meier, R. Shapira-Frommer, T. Safra, D. Matei, E. Macpherson, C. Watkins, J. Carmichael, U. Matulonis, Olaparib maintenance therapy in platinum-sensitive relapsed ovarian cancer, N Engl J Med, 366 (2012) 1382-1392.
[5] M.R. Mirza, B.J. Monk, J. Herrstedt, A.M. Oza, S. Mahner, A. Redondo, M. Fabbro, J.A. Ledermann, D. Lorusso, I. Vergote, N.E. Ben-Baruch, C. Marth, R. Madry, R.D. Christensen, J.S. Berek, A. Dorum, A.V. Tinker, A. du Bois, A. Gonzalez-Martin, P. Follana, B. Benigno, P. Rosenberg, L. Gilbert, B.J. Rimel, J. Buscema, J.P. Balser, S. Agarwal, U.A. Matulonis, E.-O.N. Investigators, Niraparib Maintenance Therapy in Platinum-Sensitive, Recurrent Ovarian Cancer, N Engl J Med, 375 (2016) 2154-2164.
[6] E.M. Swisher, K.K. Lin, A.M. Oza, C.L. Scott, H. Giordano, J. Sun, G.E. Konecny, R.L. Coleman, A.V. Tinker, D.M. O'Malley, R.S. Kristeleit, L. Ma, K.M. Bell-McGuinn, J.D. Brenton, J.M. Cragun, A. Oaknin, I. Ray-Coquard, M.I. Harrell, E. Mann, S.H. Kaufmann, A. Floquet, A. Leary, T.C. Harding, S. Goble, L. Maloney, J. Isaacson, A.R. Allen, L. Rolfe, R. Yelensky, M. Raponi, I.A. McNeish, Rucaparib in relapsed, platinum-sensitive high-grade ovarian carcinoma (ARIEL2 Part 1): an international, multicentre, open-label, phase 2 trial, Lancet Oncol, 18 (2017) 75-87.
[7] C.J. Lord, A.N. Tutt, A. Ashworth, Synthetic lethality and cancer therapy: lessons learned from the development of PARP inhibitors, Annu Rev Med, 66 (2015) 455-470.
[8] K.W. Caldecott, XRCC1 and DNA strand break repair, DNA Repair (Amst), 2 (2003) 955-969.
[9] R.E. London, The structural basis of XRCC1-mediated DNA repair, DNA Repair (Amst), 30 (2015) 90-103.
[10] N.C. Hoch, H. Hanzlikova, S.L. Rulten, M. Tetreault, E. Komulainen, L. Ju, P. Hornyak, Z. Zeng, W. Gittens, S.A. Rey, K. Staras, G.M. Mancini, P.J. McKinnon, Z.Q. Wang, J.D. Wagner, C. Care4Rare Canada, G. Yoon, K.W. Caldecott, XRCC1 mutation is associated with PARP1 hyperactivation and cerebellar ataxia, Nature, 541 (2017) 87-91.
[11] T. Abdel-Fatah, R. Sultana, R. Abbotts, C. Hawkes, C. Seedhouse, S. Chan, S. Madhusudan, Clinicopathological and functional significance of XRCC1 expression in ovarian cancer, Int J Cancer, 132 (2013) 2778-2786.
[12] C.M. Beaufort, J.C. Helmijr, A.M. Piskorz, M. Hoogstraat, K. Ruigrok-Ritstier, N. Besselink, M. Murtaza, I.W.F. van, A.A. Heine, M. Smid, M.J. Koudijs, J.D. Brenton, E.M. Berns, J. Helleman, Ovarian cancer cell line panel (OCCP): clinical importance of in vitro morphological subtypes, PLoS One, 9 (2014) e103988.
[13] E. Gogola, A.A. Duarte, J.R. de Ruiter, W.W. Wiegant, J.A. Schmid, R. de Bruijn, D.I. James, S. Guerrero Llobet, D.J. Vis, S. Annunziato, B. van den Broek, M. Barazas, A. Kersbergen, M. van de Ven, M. Tarsounas, D.J. Ogilvie, M. van Vugt, L.F.A. Wessels, J. Bartkova, I. Gromova, M. Andujar-Sanchez, J. Bartek, M. Lopes, H. van Attikum, P. Borst, J. Jonkers, S. Rottenberg, Selective Loss of PARG Restores PARylation and Counteracts PARP Inhibitor-Mediated Synthetic Lethality, Cancer Cell, 33 (2018) 1078-1093 e1012.
[14] D.W. Koh, V.L. Dawson, T.M. Dawson, The road to survival goes through PARG, Cell Cycle, 4 (2005) 397-399.
[15] W. Min, Z.Q. Wang, Poly (ADP-ribose) glycohydrolase (PARG) and its therapeutic potential, Front Biosci (Landmark Ed), 14 (2009) 1619-1626.

[16] C. Fathers, R.M. Drayton, S. Solovieva, H.E. Bryant, Inhibition of poly(ADP-ribose) glycohydrolase (PARG) specifically kills BRCA2-deficient tumor cells, Cell Cycle, 11 (2012) 990-997.
[17] P. Gravells, E. Grant, K.M. Smith, D.I. James, H.E. Bryant, Specific killing of DNA damage-response deficient cells with inhibitors of poly(ADP-ribose) glycohydrolase, DNA Repair (Amst), 52 (2017) 81-91.
[18] M. Bhandaru, M. Martinka, G. Li, A. Rotte, Loss of XRCC1 confers a metastatic phenotype to melanoma cells and is associated with poor survival in patients with melanoma, Pigment Cell Melanoma Res, 27 (2014) 366-375.
[19] Q.H. Liu, Y. Wang, H.M. Yong, P.F. Hou, J. Pan, J. Bai, J.N. Zheng, XRCC1 serves as a potential prognostic indicator for clear cell renal cell carcinoma and inhibits its invasion and metastasis through suppressing MMP-2 and MMP-9, Oncotarget, 8 (2017) 109382-109392.
[20] Y.G. Wang, T.Y. Zheng, XRCC1-77T>C polymorphism and cancer risk: a meta-analysis, Asian Pac J Cancer Prev, 13 (2012) 111-115.
[21] N.N. Yang, Y.F. Huang, J. Sun, Y. Chen, Z.M. Tang, J.F. Jiang, Meta-analysis of XRCC1 polymorphism and risk of female reproductive system cancer, Oncotarget, 8 (2017) 28455-28462.
[22] Z. Zhang, Q. Xiang, G. Mu, Q. Xie, S. Chen, S. Zhou, K. Hu, Y.M. Cui, XRCC1 polymorphism and overall survival in ovarian cancer patients treated with platinum-based chemotherapy: A systematic review and MOOSE-compliant meta-analysis, Medicine (Baltimore), 97 (2018) e12996.
[23] D.Q. Zhu, Q. Zou, C.H. Hu, J.L. Su, G.H. Zhou, P. Liu, XRCC1 genetic polymorphism acts a potential biomarker for lung cancer, Tumour Biol, 36 (2015) 3745-3750.
[24] A. Gan, A.R. Green, C.C. Nolan, S. Martin, S. Deen, Poly(adenosine diphosphate-ribose) polymerase expression in BRCA-proficient ovarian high-grade serous carcinoma; association with patient survival, Hum Pathol, 44 (2013) 1638-1647.
[25] W.Z. Wysham, P. Mhawech-Fauceglia, H. Li, L. Hays, S. Syriac, T. Skrepnik, J. Wright, N. Pande, M. Hoatlin, T. Pejovic, BRCAness profile of sporadic ovarian cancer predicts disease recurrence, PLoS One, 7 (2012) e30042.
[26] M. Masson, C. Niedergang, V. Schreiber, S. Muller, J. Menissier-de Murcia, G. de Murcia, XRCC1 is specifically associated with poly(ADP-ribose) polymerase and negatively regulates its activity following DNA damage, Mol Cell Biol, 18 (1998) 3563-3571.
[27] E.H. Stover, P.A. Konstantinopoulos, U.A. Matulonis, E.M. Swisher, Biomarkers of Response and Resistance to DNA Repair Targeted Therapies, Clin Cancer Res, 22 (2016) 5651-5660.
[28] C.J. Lord, S. McDonald, S. Swift, N.C. Turner, A. Ashworth, A high-throughput RNA interference screen for DNA repair determinants of PARP inhibitor sensitivity, DNA Repair (Amst), 7 (2008) 2010-2019.
[29] J.K. Horton, D.F. Stefanick, R. Prasad, N.R. Gassman, P.S. Kedar, S.H. Wilson, Base excision repair defects invoke hypersensitivity to PARP inhibition, Mol Cancer Res, 12 (2014) 1128-1139.
[30] R. Ali, A. Al-Kawaz, M.S. Toss, A.R. Green, I.M. Miligy, K.A. Mesquita, C. Seedhouse, S. Mirza, V. Band, E.A. Rakha, S. Madhusudan, Targeting PARP1 in XRCC1-Deficient Sporadic Invasive Breast Cancer or Preinvasive Ductal Carcinoma In Situ Induces Synthetic Lethality and Chemoprevention, Cancer Res, 78 (2018) 6818-6827.
[31] K. Zaniolo, S. Desnoyers, S. Leclerc, S.L. Guerin, Regulation of poly(ADP-ribose) polymerase-1 (PARP-1) gene expression through the post-translational modification of Sp1: a nuclear target protein of PARP-1, BMC Mol Biol, 8 (2007) 96.
[32] Martin L. , T. Tzuling Cheng, Dominic I. James D.I., Begum H., Smith K.M., Jordan A., Waddell I., Vaidya K., Fischer M., Yao B., JDrummond J., Cleary L., Martinez R., Sutton J., Ravindran N., Joseph J., Venetsanakos E., Dillon M., H. J.H., B. L.D., PARG inhibitors exhibit synthetic lethality with XRCC1 deficiency and a cellular mechanism of action that is distinct from PARP inhibition, Cancer Res, DOI: 10.1158/1538-7445.AM2018-1943 (2018).

[33] N. Pillay, A. Tighe, L. Nelson, S. Littler, C. Coulson-Gilmer, N. Bah, A. Golder, B. Bakker, D.C.J. Spierings, D.I. James, K.M. Smith, A.M. Jordan, R.D. Morgan, D.J. Ogilvie, F. Foijer, D.A. Jackson, S.S. Taylor, DNA Replication Vulnerabilities Render Ovarian Cancer Cells Sensitive to Poly(ADP-Ribose) Glycohydrolase Inhibitors, Cancer Cell, 35 (2019) 519-533 e518.

FIGURE LEGENDS

Figure 1: Prognostic and predictive significance of XRCC1 and PARP1 expression in ovarian cancers. (**A)** Representative photomicrographic images of XRCC1 and PARP1 immunohistochemical expression in ovarian tissue microarrays. **(B)** Kaplan Meier curves for XRCC1 protein expression showing progression free survival (PFS). (**C)** Kaplan Meier curves for PARP1 protein expression showing progression free survival (PFS). (**D)** Kaplan Meier curves for XRCC1-PARP1 co-expression showing progression free survival (PFS). (**E)** Kaplan Meier curves for XRCC1 showing overall survival (OCSS). (**F)** Kaplan Meier curves for PARP1 showing OCSS. (**G)** Kaplan Meier curves for XRCC1-PARP1 co-expression showing OCSS.

Figure 2: XRCC1 deficiency and Olaparib induced synthetic lethality. (**A)** Clonogenic survival assay for cisplatin sensitivity in A2780 and A2780cis cells. **(B)** Western blot of XRCC1 levels in A2780 and A2780cis transfected with XRCC1 siRNA or scrambled siRNA control. **(C)** Western blot of PARP1 and quantification in A2780, A2780cis control and XRCC1 knock down. **(D)** Clonogenic survival assay for A2780, A2780cis control and XRCC1 knock down treated with different doses of Olaparib. Cells were plated overnight and then transfected with XRCC1 siRNA or scrambled siRNA control. On day two, cells were trypsinized, collected and re-plated in 6-well plates for clonogenic assays. On day three, cells were treated with indicated doses of Olaparib. For Flow cytometry analysis, transfected cells were plated on day two overnight and then treated with 10μM of Olaparib for 24 hrs. **(E)** Quantification of γH2AX levels by flow cytometry in untreated (UT) or Olaparib treated (10μM) control and XRCC1_KD cells. **(F)** Quantification of cell cycle progression by flow cytometry in untreated (UT) or Olaparib treated (10μM) control and XRCC1_KD cells. **(G)**

Quantification of apoptotic cells by Annexin V flow cytometry in untreated (UT) or Olaparib treated (10μM) cells control and XRCC1_KD cells. **(H)** Clonogenic survival assay for OVCAR3 scrambled control and OVCAR3(XRCC1_KD) cells in different doses of Olaparib. **(I)** Clonogenic survival assay for OVCAR4 scrambled control and OVCAR4(XRCC1_KD) cells in different doses of Olaparib**. (J)** Clonogenic survival assay for PE04 scrambled control and PE04 (XRCC1_KD) cells in different doses of Olaparib. **(K)** Clonogenic survival assay for SKOV3 scrambled control and SKOV3(XRCC1_KD) cells in different doses of Olaparib. All figures are representative of 3 or more independent experiments. P values are indicated as follows; **'*'** $p<0.05$, '**' $p<0.01$, '***' $p<0.001$. Error bar indicates standard error of mean.

Figure 3: PARP1 inhibitor sensitivity in A2780 XRCC1 knock out cells. **(A)** Western blot showing XRCC1koock out in A2780 using CRISPR-Cas9 methodology. **(B)** Clonogenic survival assay for A2780 control and A2780 XRCC1_KO cells in different doses of Olaparib. **(C)** Clonogenic survival assay for A2780 control and A2780 XRCC1_KO cells in different doses of Talazoparib. (D) Representative photomicrographic images of 53BP1 and γH2AX immunofluorescence staining in A2780 cantrol and XRCC1_KO cells treated with Olaparib (10μM) or Talazoparib (5μM) for 24 h. (E) Quantification of 53BP1 and γH2AX mean fluorescence intensity by ImageJ software. For analysis minimum of 100 cells were counted. All figures are representative of 3 or more independent experiments. P values are indicated as follows; **'*'** $p<0.05$, '**' $p<0.01$, '***' $p<0.001$. Error bar indicates standard error of mean.

Figure 4: Functional studies of PARP1 inhibitor induced synthetic lethality in A2780 XRCC1_KO cells. **(A)** Quantification of γH2AX levels by flow cytometry in untreated (UT) or Olaparib treated (10μM) A2780 control and XRCC1_KO cells. **(B)** Quantification of cell cycle progression by flow cytometry in untreated (UT) or Olaparib treated (10μM) A2780

control and XRCC1_KO cells. **(C**) Quantification of apoptotic cells by Annexin V flow cytometry in untreated (UT) or Olaparib treated (10µM) A2780 control and XRCC1_KO cells. **(D)** Quantification of γH2AX levels by flow cytometry in untreated (UT) or Talazoparib treated (5 µM) A2780 control and XRCC1_KO cells. **(E)** Quantification of cell cycle progression by flow cytometry in untreated (UT) or Talazoparib treated (5µM) A2780 control and XRCC1_KO cells. **(F**) Quantification of apoptotic cells by Annexin V flow cytometry in untreated (UT) or Talazoparib treated (5µM) A2780 control and XRCC1_KO cells.

Figure 5: PARP1 inhibitor or PARG inhibitor sensitivity in XRCC1 Knockout (KO) cells. **(A)** Clonogenic survival assay of A2780 control and XRCC1 knock out treated with the indicated doses of PDD00017273**. (B)** Quantification of γH2AX levels by flow cytometry in untreated (UT) or PDD00017273 treated (10 µM) A2780 control and XRCC1_KO cells. **(C)** Quantification of cell cycle progression by flow cytometry in untreated (UT) or PDD00017273 treated (10 µM) A2780 control and XRCC1_KO cells. **(D**) Quantification of apoptotic cells by Annexin V flow cytometry in untreated (UT) or PDD00017273 treated (10 µM) A2780 control and XRCC1_KO cells **. (E)** Representative photomicrographic images of A2780 control and XRCC1_KO 3D spheres treated with Olaparib (10µM), Talazoparib (5µM), and PDD00017273 (10µM). Quantification of viable, dead cells by flow cytometry in: A2780control **(F)** and A2780 (XRCC1_KO) **(G)** treated with Olaparib, Talazoparib and PD00017273**.** See methods for further details. All figures are representative of 3 or more independent experiments. P values are indicated as follows; **'*'** $p<0.05$, '**' $p<0.01$, '***' $p<0.001$. Error bar indicates standard error of mean.

Figure 6: (A) Representative images for migration assay in A2780 control and A2780(XRCC1_KO) cells. CytochalasinD (1.5μM) was used as a negative control. Quantification was performed in ImageJ software. **(B)** Representative images for invasion assay and quantification in A2780 control and A2780 (XRCC1_KO) cells. P values are indicated as follows; **'*'** $p<0.05$, '**' $p<0.01$, '***' $p<0.001$. Error bar indicates standard error of mean. **(C)** Kaplan Meier curves for BRCA2-XRCC1 co-expression showing PFS. **(D)** Kaplan Meier curves for BRCA2-XRCC1 co-expression showing OS.

Figure 1

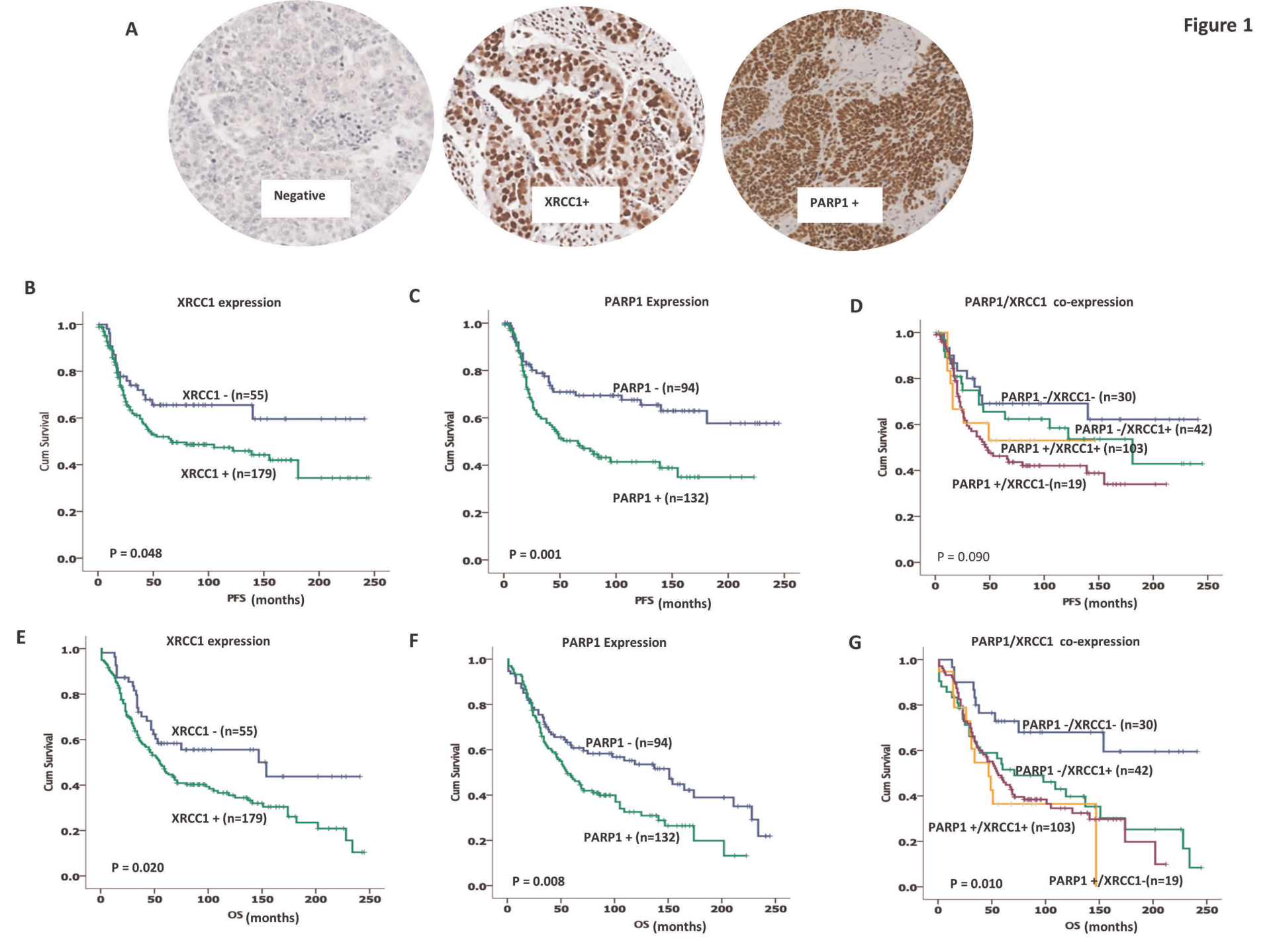
A
Negative
XRCC1+
PARP1 +
B
XRCC1 expression
XRCC1 - (n=55)
XRCC1 + (n=179)
P = 0.048
Cum Survival
PFS (months)
C
PARP1 Expression
PARP1 - (n=94)
PARP1 + (n=132)
P = 0.001
Cum Survival
PFS (months)
D
PARP1/XRCC1 co-expression
PARP1 -/XRCC1- (n=30)
PARP1 -/XRCC1+ (n=42)
PARP1 +/XRCC1+ (n=103)
PARP1 +/XRCC1-(n=19)
P = 0.090
Cum Survival
PFS (months)
E
XRCC1 expression
XRCC1 - (n=55)
XRCC1 + (n=179)
P = 0.020
Cum Survival
OS (months)
F
PARP1 Expression
PARP1 - (n=94)
PARP1 + (n=132)
P = 0.008
Cum Survival
OS (months)
G
PARP1/XRCC1 co-expression
PARP1 -/XRCC1- (n=30)
PARP1 -/XRCC1+ (n=42)
PARP1 +/XRCC1+ (n=103)
PARP1 +/XRCC1-(n=19)
P = 0.010
Cum Survival
OS (months)

Figure 2

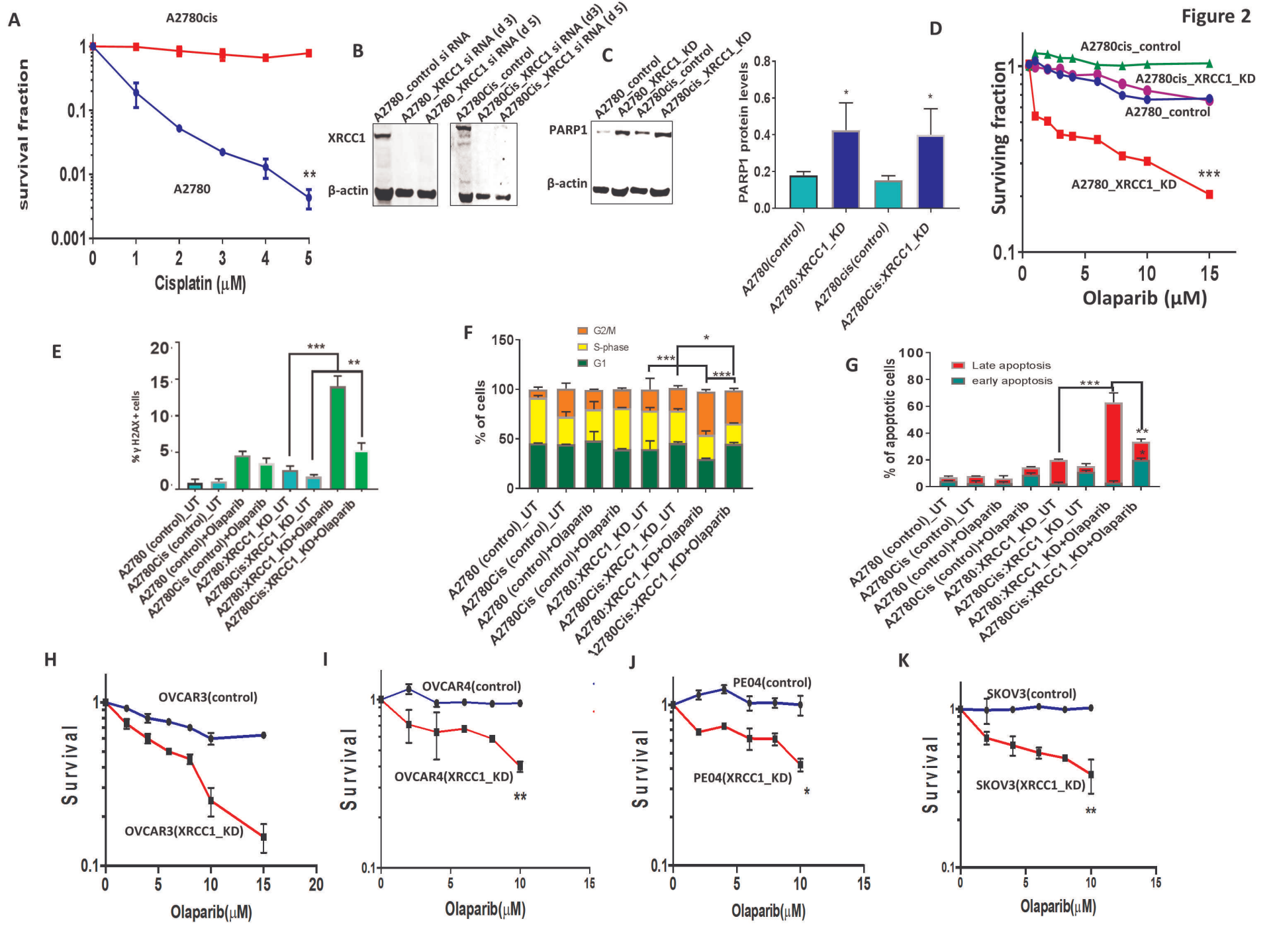
A
A2780cis
survival fraction
A2780
**
Cisplatin (μM)
B
A2780_control si RNA
A2780_XRCC1 si RNA (d 3)
A2780_XRCC1 si RNA (d 5)
A2780cis_control
A2780cis_XRCC1 si RNA (d3)
A2780cis_XRCC1 si RNA (d 5)
XRCC1
β-actin
C
A2780_control
A2780_XRCC1_KD
A2780cis_control
A2780cis_XRCC1_KD
PARP1
β-actin
PARP1 protein levels
A2780(control)
A2780:XRCC1_KD
A2780cis(control)
A2780Cis:XRCC1_KD
D
A2780cis_control
A2780cis_XRCC1_KD
A2780_control
A2780_XRCC1_KD
***
Surviving fraction
Olaparib (μM)
E
% γ H2AX + cells
***
**
A2780 (control)_UT
A2780Cis (control)_UT
A2780 (control)+Olaparib
A2780Cis (control)+Olaparib
A2780:XRCC1_KD_UT
A2780Cis:XRCC1_KD_UT
A2780:XRCC1_KD+Olaparib
A2780Cis:XRCC1_KD+Olaparib
F
G2/M
S-phase
G1
% of cells
***
*
***
A2780 (control)_UT
A2780Cis (control)_UT
A2780 (control)+Olaparib
A2780Cis (control)+Olaparib
A2780:XRCC1_KD_UT
A2780Cis:XRCC1_KD_UT
A2780:XRCC1_KD+Olaparib
A2780Cis:XRCC1_KD+Olaparib
G
Late apoptosis
early apoptosis
% of apoptotic cells
***
**
A2780 (control)_UT
A2780Cis (control)_UT
A2780 (control)+Olaparib
A2780Cis (control)+Olaparib
A2780:XRCC1_KD_UT
A2780Cis:XRCC1_KD_UT
A2780:XRCC1_KD+Olaparib
A2780Cis:XRCC1_KD+Olaparib
H
OVCAR3(control)
Survival
OVCAR3(XRCC1_KD)
Olaparib(μM)
I
OVCAR4(control)
Survival
OVCAR4(XRCC1_KD)
**
Olaparib(μM)
J
PE04(control)
Survival
PE04(XRCC1_KD)
*
Olaparib(μM)
K
SKOV3(control)
Survival
SKOV3(XRCC1_KD)
**
Olaparib(μM)

Figure 3

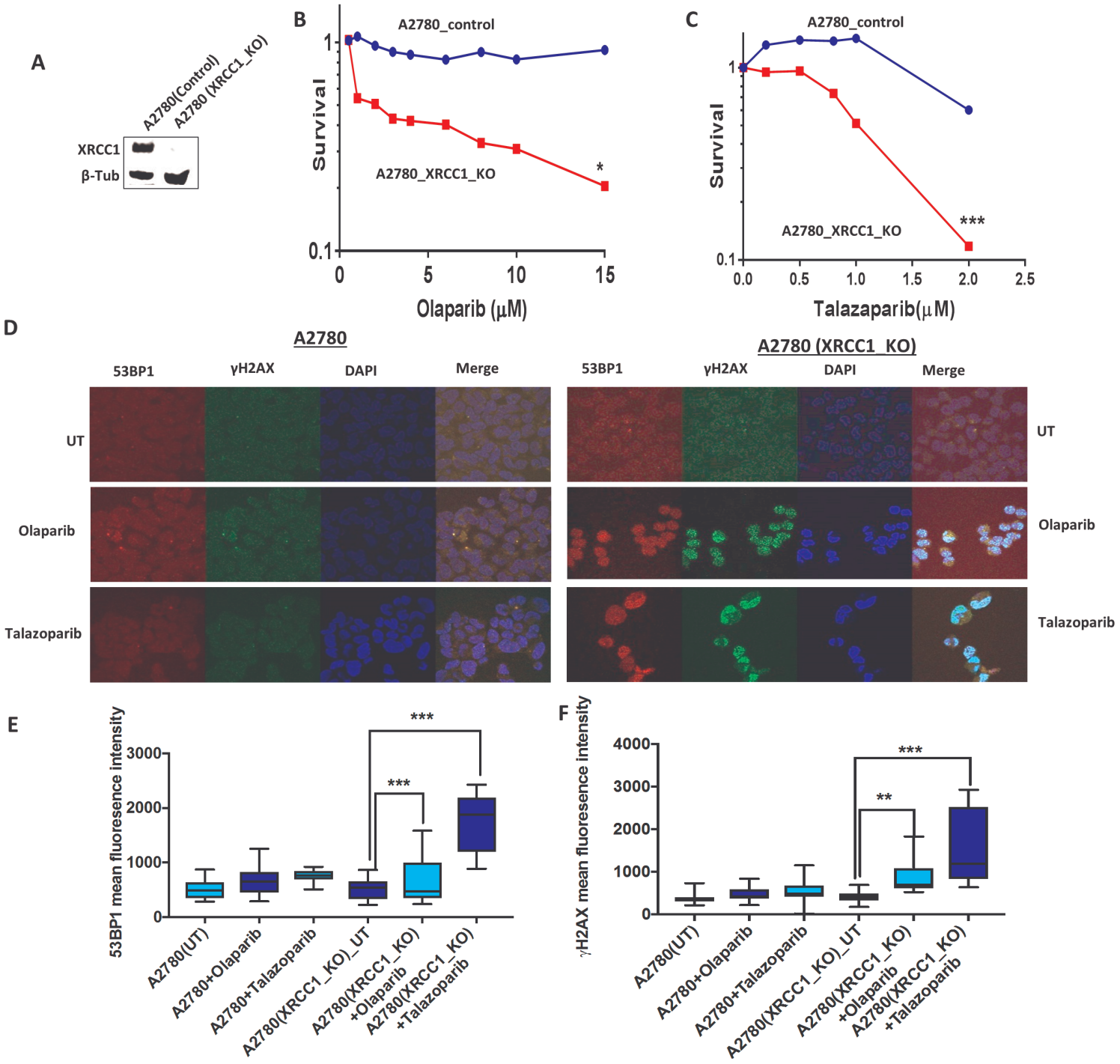
A
A2780(Control)
A2780 (XRCC1_KO)
XRCC1
β-Tub
B
A2780_control
A2780_XRCC1_KO
Survival
Olaparib (μM)
C
A2780_control
A2780_XRCC1_KO
Survival
Talazaparib(μM)
D
A2780
A2780 (XRCC1_KO)
53BP1
γH2AX
DAPI
Merge
UT
Olaparib
Talazoparib
E
53BP1 mean fluoresence intensity
A2780(UT)
A2780+Olaparib
A2780+Talazoparib
A2780(XRCC1_KO)_UT
A2780(XRCC1_KO) +Olaparib
A2780(XRCC1_KO) +Talazoparib
F
γH2AX mean fluoresence intensity

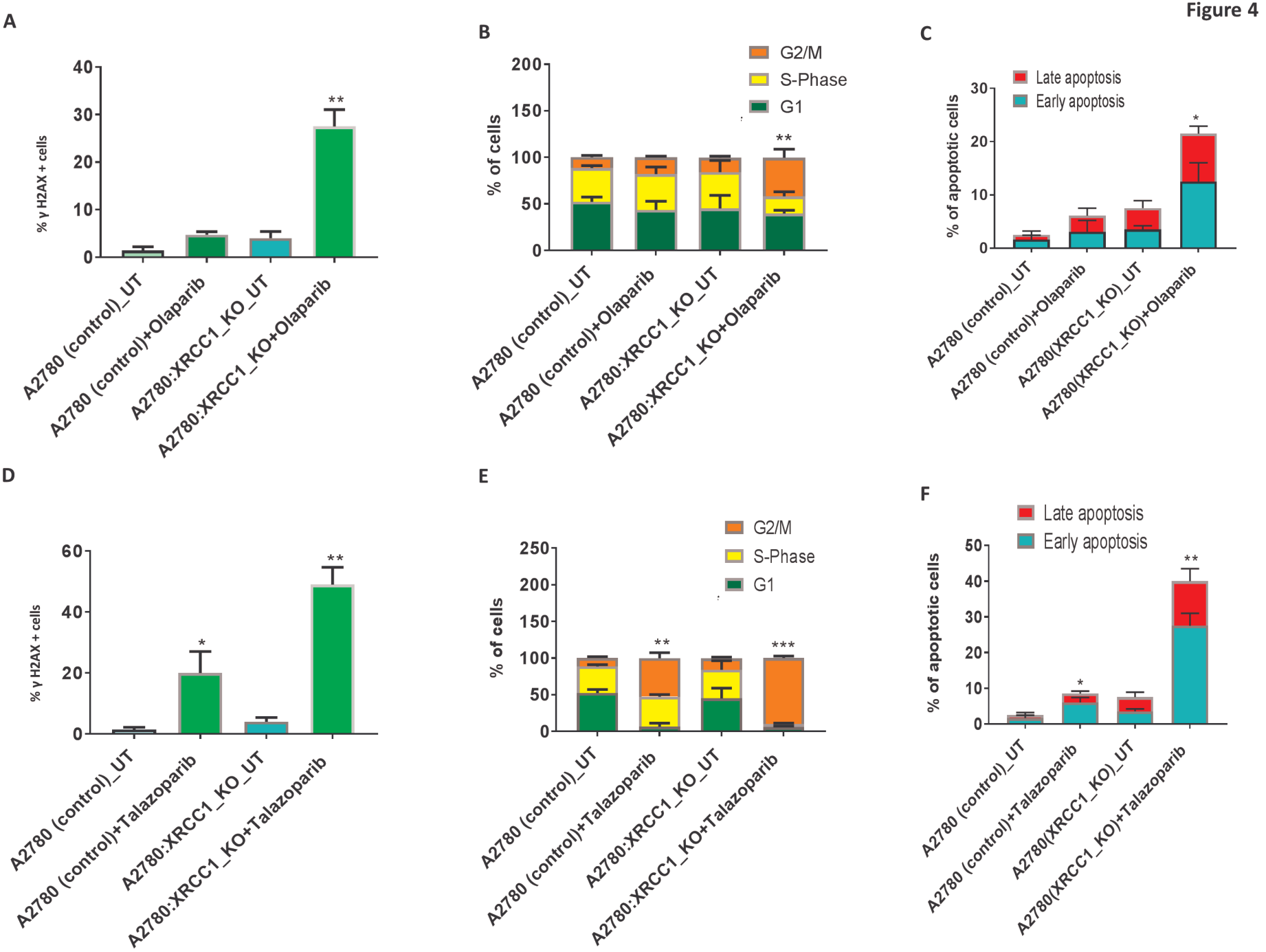
A
% γ H2AX + cells
40
30
20
10
0
**
A2780 (control)_UT
A2780 (control)+Olaparib
A2780:XRCC1_KO_UT
A2780:XRCC1_KO+Olaparib
B
% of cells
200
150
100
50
0
G2/M
S-Phase
G1
**
A2780 (control)_UT
A2780 (control)+Olaparib
A2780:XRCC1_KO_UT
A2780:XRCC1_KO+Olaparib
C
% of apoptotic cells
30
20
10
0
Late apoptosis
Early apoptosis
*
A2780 (control)_UT
A2780 (control)+Olaparib
A2780(XRCC1_KO)_UT
A2780(XRCC1_KO)+Olaparib
D
% γ H2AX + cells
60
40
20
0
*
**
A2780 (control)_UT
A2780 (control)+Talazoparib
A2780:XRCC1_KO_UT
A2780:XRCC1_KO+Talazoparib
E
% of cells
250
200
150
100
50
0
G2/M
S-Phase
G1
**
***
A2780 (control)_UT
A2780 (control)+Talazoparib
A2780:XRCC1_KO_UT
A2780:XRCC1_KO+Talazoparib
F
% of apoptotic cells
50
40
30
20
10
0
Late apoptosis
Early apoptosis
*
**
A2780 (control)_UT
A2780 (control)+Talazoparib
A2780(XRCC1_KO)_UT
A2780(XRCC1_KO)+Talazoparib

Figure 5

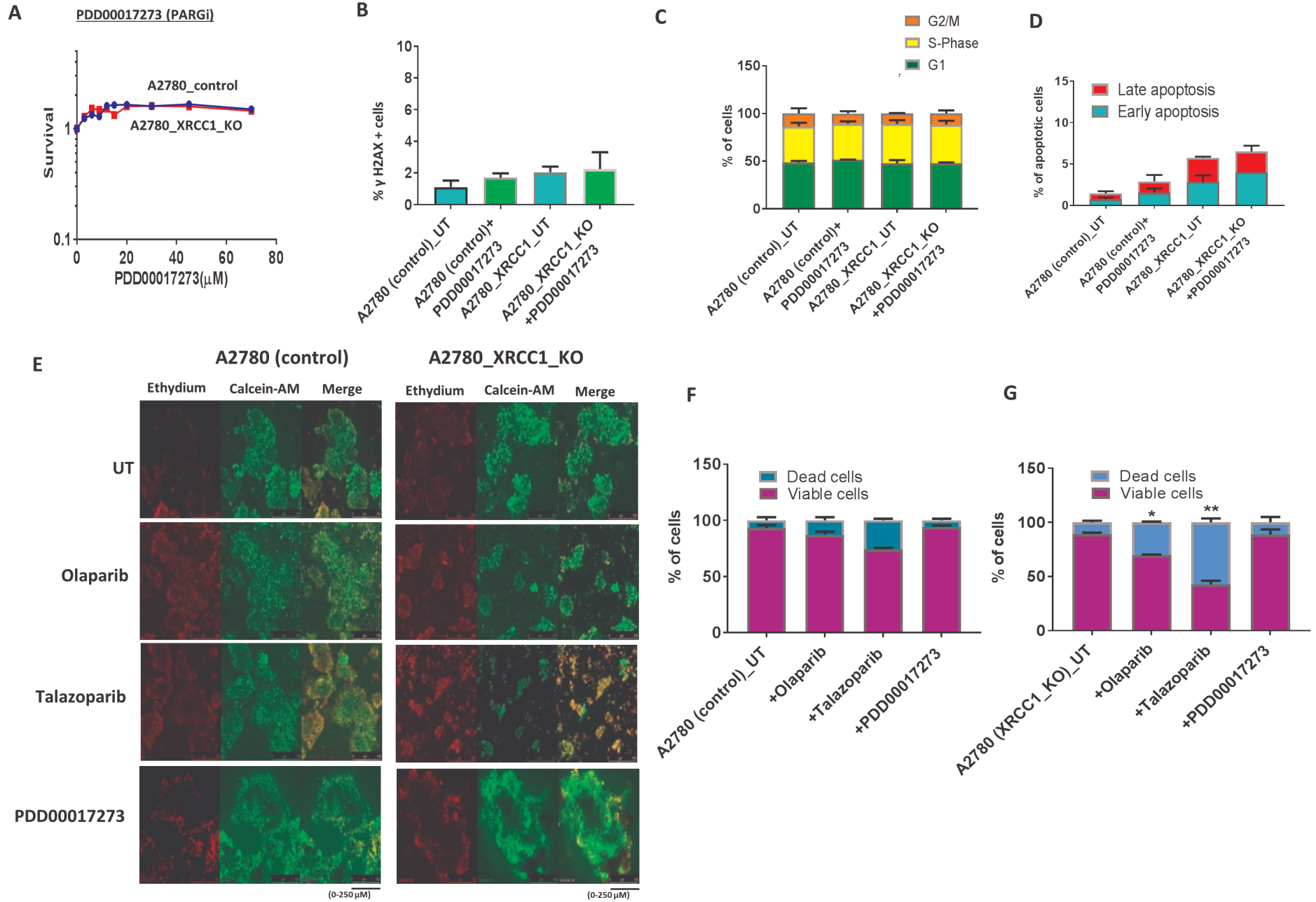
A
PDD00017273 (PARGi)
Survival
A2780_control
A2780_XRCC1_KO
PDD00017273(μM)
B
% γ H2AX + cells
A2780 (control)_UT
A2780 (control)+ PDD00017273
A2780_XRCC1_UT
A2780_XRCC1_KO +PDD00017273
C
G2/M
S-Phase
G1
% of cells
D
Late apoptosis
Early apoptosis
% of apoptotic cells
E
A2780 (control)
A2780_XRCC1_KO
Ethydium
Calcein-AM
Merge
UT
Olaparib
Talazoparib
PDD00017273
(0-250 μM)
F
Dead cells
Viable cells
% of cells
A2780 (control)_UT
+Olaparib
+Talazoparib
+PDD00017273
G
A2780 (XRCC1_KO)_UT

A

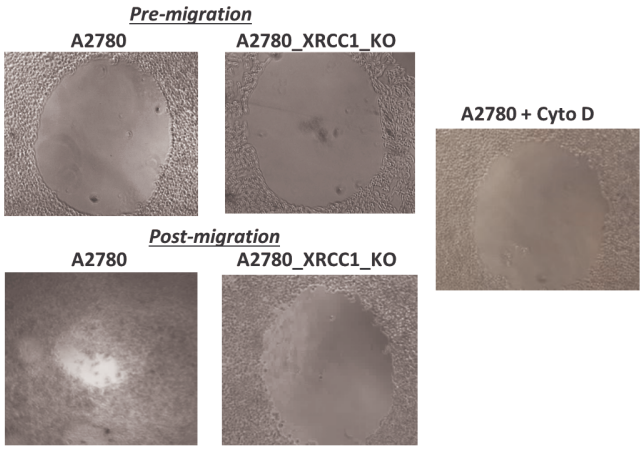
Pre-migration
A2780
A2780_XRCC1_KO
A2780 + Cyto D
Post-migration
A2780
A2780_XRCC1_KO

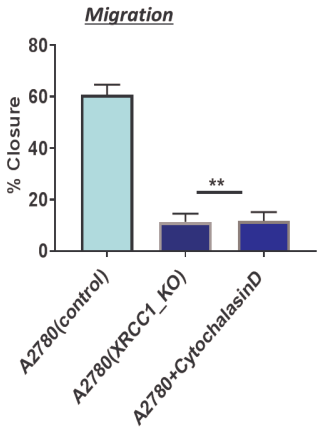
Migration
% Closure
80
60
40
20
0
**
A2780(control)
A2780(XRCC1_KO)
A2780+CytochalasinD

B

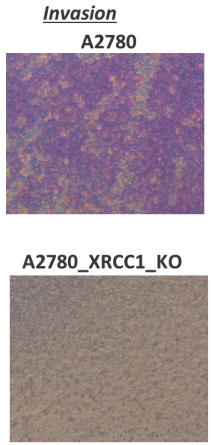
Invasion
A2780
A2780_XRCC1_KO

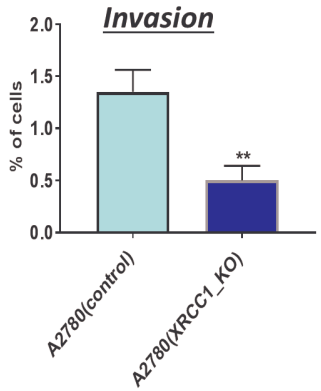
Invasion
% of cells
2.0
1.5
1.0
0.5
0.0
**
A2780(control)
A2780(XRCC1_KO)

C

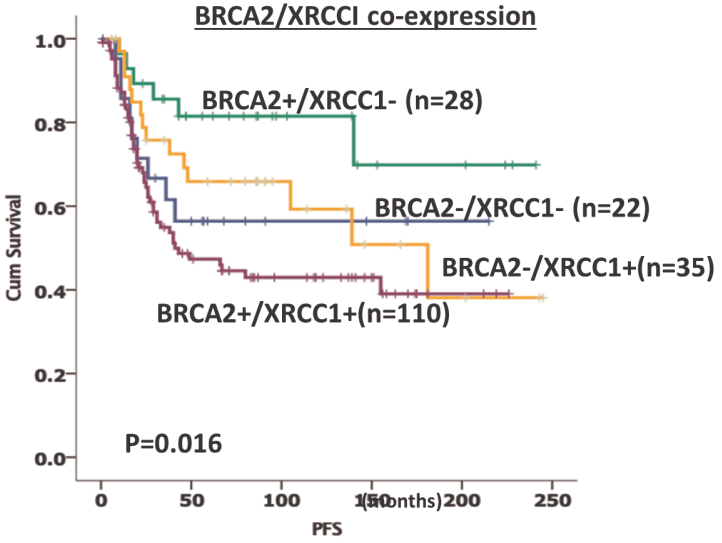
BRCA2/XRCCI co-expression
Cum Survival
1.0
0.8
0.6
0.4
0.2
0.0
BRCA2+/XRCC1- (n=28)
BRCA2-/XRCC1- (n=22)
BRCA2-/XRCC1+(n=35)
BRCA2+/XRCC1+(n=110)
P=0.016
0
50
100
150
200
250
(months)
PFS

D

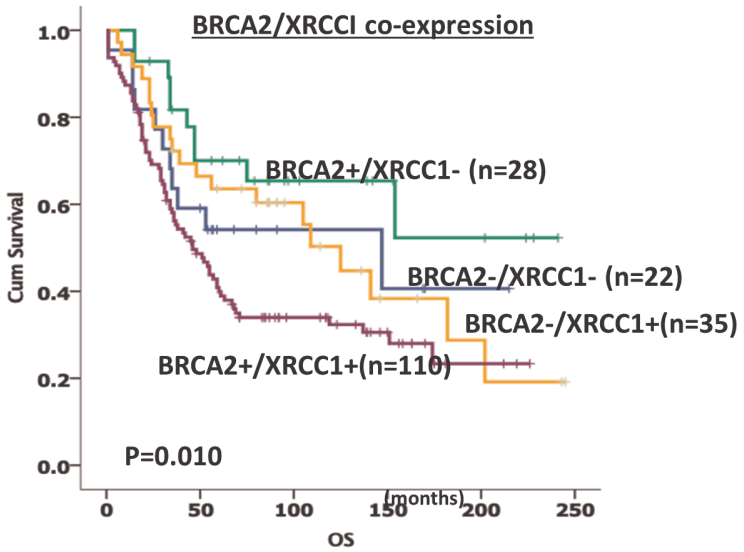
BRCA2/XRCCI co-expression
Cum Survival
1.0
0.8
0.6
0.4
0.2
0.0
BRCA2+/XRCC1- (n=28)
BRCA2-/XRCC1- (n=22)
BRCA2-/XRCC1+(n=35)
BRCA2+/XRCC1+(n=110)
P=0.010
0
50
100
150
200
250
(months)
OS

Supplementary Figure S1: (A)Representative images for cell γH2AX analysis by flow cytometry, (B) Representative images for cell cycle analysis by flow cytometry & (C) Representative images for annexinV analysis by flow cytometry in A2780 and A2780cis control and XRCC1_KD cells untreated and treated with Olaparib (10.μM).

Supplementary Figure S2: (A) Clonogenic survival assay for OVCAR4 scrambled control and OVCAR4(XRCC1_KD) cells treated with the indicated doses of Talazoparib. (B) Clonogenic survival assay for PEO4 scrambled control and PEO4(XRCC1_KD) cells treated with the indicated doses of Talazoparib. (C) Clonogenic survival assay for SKOV3 scrambled control and SKOV3(XRCC1_KD) cells treated with the indicated doses of Talazoparib. (D) Representative photomicrographic images for BRCA1/BRCA2 immunohistochemical staining in ovarian tissue microarrays.

Supplementary Figure S3: (A) Kaplan Meier curve for XRCC1 protein expression and PFS in ovarian cancers in BRCA1 low tumours. (**B)** Kaplan Meier curve for XRCC1 protein expression and OS in BRCA1 low ovarian cancers. (**C)** Kaplan Meier curve for XRCC1 protein expression and PFS in BRCA1 high ovarian cancers. (**D)** Kaplan Meier curve for XRCC1 expression and OS in BRCA1 high ovarian cancers. (**E)** Kaplan Meier curve for XRCC1 expression and PFS in BRCA2 low ovarian cancers. (**F)** Kaplan Meier curve for XRCC1 expression and OS in BRCA2 low ovarian cancers. **(G)** Kaplan Meier curve for XRCC1 expression and PFS in BRCA2 high ovarian cancers. (**H)** Kaplan Meier curve for XRCC1 expression and OS in BRCA2 high ovarian cancers.

Supplementary Figure S4: (A) Kaplan Meier curves for BRCA1-XRCC1 co-expression showing PFS. (**B)** Kaplan Meier curves for BRCA1-XRCC1 co-expression showing OS.

Supplementary Table S1: Patient demographics

Characteristics	**Number**	**Percentages**
Pathology		
Serous cystadenocarcinoma	290	55.2%
Endometrioid	82	15.6%
Clear cell carcinoma	48	9.1%
Mucinous cystadenocarcinoma	60	11.4%
Others	18	3.4%
Mixed	17	3.2%
Unknown	10	2.1%
Grade		
1	68	12.9%
2	87	16.5%
3	306	58.2%
Unknown	64	12.4%
Residual tumour		
None/Microscopic	265	50.4%
<1cm	82	15.6%
>1-2 cm	29	5.5%
>2cm	110	20.9%
FIGO Stage		
I	182	34.6%
II	76	14.4%
III	213	40.5%
IV	32	6%

Unknown	22	4.5%
Chemotherapy		
Carboplatin monotherapy	163	31%
Carboplatin + Paclitaxel	177	34%
Other platinum based regimes*	121	23%
No chemotherapy	25	5%
Unknown	39	7%
Platinum sensitivity		
Sensitive	376	71.6%
Resistant	85	16.1%
Unknown	64	11.8%
Relapse status		
Progression-free	238	45.3%
Progressed/relapsed	243	46.2%
Unknown	44	8.3%
Survival status		
Living	199	37.9%
Dead	286	54.4%
Unknown	40	7.6%

*= CAP (Cyclophosphamide, Adriamycin and Cisplatin), ICON5 Trial, SOCTROC Trial, Carboplatin and Endoxan

Supplementary Table S2: Clinicopathological significance of XRCC1 expression in Ovarian Cancers.

	XRCC1- N(%)	XRCC1+ N(%)	**P- value**
Pathological Type			**<0.00001**
Serous cystadenocarcinoma	66 (24.7)	201 (75.3)	
Mucinous cystadenocarcinoma	23 (47.9)	25 (52.1)	
Endometrioid	30 (41.7)	42 (58.3)	
Clear cell carcinoma	24 (58.5)	17 (41.5)	
Mixed	4 (28.6)	10 (71.4)	
FIGO Stage			**0.001**
I	70 (44.9)	86 (55.1)	
II	18 (26.5)	50 (73.5)	
III	58 (29.7)	137 (70.3)	
IV	5 (16.7)	25 (83.3)	
Tumour Grade			0.105
G1	27 (46.6)	31 (53.4)	
G2	24 (31.6)	52 (68.4)	
G3	90 (32.5)	187 (67.5)	
Measurable Disease pre-Chemotherapy			**0.002**
No measurable disease	111 (39.6)	169 (60.4)	
Measurable disease	35 (24.6)	107 (75.4)	
Platinum response			**0.003**
Sensitive	127 (38.6)	202 (61.4)	
Resistant*	17 (21.8)	61 (78.2)	

FIGO= International Federation of Obstetricians and Gynaecologists (FIGO) Staging System for Ovarian Cancer

G= tumour grade

* = Platinum resistance was defined as patients who had progression during first-line platinum chemotherapy or relapse within 6 months after completion of chemotherapy

Supplementary Table S3: PARP1 and Ovarian Cancer

	PARP1- N(%)	**PARP1+ N(%)**	**P- value**
Pathological Type			**<0.00001**
Serous cystadenocarcinoma	84 (35.7)	151 (64.3)	
Mucinous cystadenocarcinoma	37 (78.7)	10 (21.3)	
Endometrioid	40 (58.0)	29 (42.0)	
Clear cell carcinoma	29 (80.6)	7 (19.4)	
Mixed	3 (21.4)	11 (78.6)	
FIGO Stage			0.443
I	78 (52.3)	71 (47.7)	
II	29 (44.6)	36 (55.4)	
III	74 (43.5)	96 (56.5)	
IV	12 (48.0)	13 (52.0)	
Tumour Grade			**<0.00001**
G1	43 (75.4)	14 (24.6)	
G2	31 (46.3)	36 (53.7)	
G3	104 (41.8)	145 (58.2)	
Measurable Disease pre-chemotherapy			**0.024**
No measurable disease	138 (52.1)	127 (47.9)	
Measurable disease	48 (39.7)	73 (60.3)	

Supplementary Table S4: PARP1/XRCC1 co-expression and Ovarian Cancer

	PARP1-/ XRCC1- N(%)	**PARP1-/ XRCC1+ N(%)**	**PARP1+/ XRCC1 - N(%)**	**PARP1+/ XRCC1 + N(%)**	**P- value**
Pathological Type					***<0.0001***
Serous cystadenocarcinoma	32 (14.3)	45 (20.2)	27 (12.1)	119 (53.4)	
Mucinous cystadenocarcinoma	18 (45.0)	14 (35.0)	1 (2.5)	7 (17.5)	
Endometrioid	21 (34.4)	14 (23.0)	6 (9.8)	20 (32.8)	
Clear cell carcinoma	19 (59.4)	7 (21.9)	1 (3.1)	5 (15.6)	
Mixed	1 (7.7)	2 (15.4)	3 (23.1)	7 (53.8)	
FIGO Stage					0.100
I	46 (34.3)	22 (16.4)	13 (9.7)	53 (39.6)	
II	11 (18.3)	14 (23.3)	7 (11.7)	28 (46.7)	
III	30 (18.9)	40 (25.2)	20 (12.6)	69 (43.4)	
IV	4 (16.7)	7 (29.2)	1 (4.2)	12 (50.0)	
Tumour Grade					***0.002***
G1	22 (44.0)	15 (30.0)	1 (2.0)	12 (24.0)	
G2	15 (24.2)	13 (21.0)	7 (11.3)	27 (43.5)	
G3	48 (20.6)	47 (20.2)	30 (12.9)	108 (46.4)	
Measurable Disease Before ChemoTherapy					***0.004***
No measurable disease	73 (30.5)	47 (19.7)	23 (9.6)	96 (40.2)	
Measurable disease	15 (13.0)	30 (26.1)	16 (13.9)	54 (47.0)	

Supplementary Table S5. Multivariate analysis

PFS	Sig.	Exp(B)	95.0% CI for Exp(B)	
			Lower	Upper
Platinum Sensitivity	**0.0001**	13.957	9.572	20.351
XRCC1	**0.016**	1.503	1.078	2.096
PARP1	0.447	1.128	.827	1.539
OCSS				
Platinum_Sensitivity	**0.0001**	6.772	4.854	9.448
XRCC1	0.170	1.258	.906	1.748
PARP1	**0.023**	1.421	1.051	1.922

Supplementary Table S6: BRCA2 and Ovarian Cancer

	BRCA2- N (%)	BRCA2+ N (%)	**P- value**
Pathological Type			**0.005**
Serous cystadenocarcinoma	29 (21.3)	107 (78.7)	
Mucinous cystadenocarcinoma	11 (30.6)	25 (69.4)	
Endometrioid	16 (50)	16 (50)	
Clear cell carcinoma	8 (40)	12 (60)	
Mixed	1 (10)	9 (90)	
FIGO Stage			0.256
I	31 (31)	69 (69)	
II	7 (21.2)	26 (78.8)	
III	29 (30.2)	67 (69.8)	
IV	0 (0)	7 (100)	
Tumour Grade			0.403
G1	13 (35.1)	24 (64.9)	
G2	13 (28.9)	32 (71.1)	
G3	31 (24.2)	97 (75.8)	
Measurable Disease pre-Chemotherapy			0.411
No measurable disease	44 (27.7)	115 (72.3)	
Measurable disease	20 (33.3)	40 (66.7)	

Supplementary Table S7: BRCA2-XRCC1 co-expression and Ovarian Cancer

	BRCA2-/ XRCC1- N (%)	**BRCA2+/ XRCC1+ N (%)**	**BRCA2-/ XRCC1+ N (%)**	**BRCA2+/ XRCC1 + N (%)**	**P- value**
Pathological Type					***0.002***
Serous cystadenocarcinoma	6 (4.6)	14 (10.7)	21 (16)	90 (68.7)	
Mucinous cystadenocarcinoma	4 (12.9)	10 (32.3)	5 (16.1)	12 (38.7)	
Endometrioid	5 (17.2)	3 (10.3)	9 (31)	12 (41.4)	
Clear cell carcinoma	5 (27.8)	2 (11.2)	3 (16.7)	8 (44.4)	
Mixed	1 (11.1)	2 (22.2)	0 (0)	6 (66.7)	
FIGO Stage					0.05
I	10 (11)	20 (22)	17 (18.7)	44 (48.4)	
II	1 (3.2)	5 (16.1)	5 (16.1)	20 (64.5)	
III	11 (12.1)	6 (6.6)	16 (17.6)	58 (63.7)	
IV	0 (0)	0 (0)	0 (0)	7 (100.0)	
Tumour Grade					0.098
G1	4 (12.1)	9 (27.3)	7 (21.2)	13 (39.2)	
G2	3 (7)	7 (16.3)	9 (20.0)	24 (55.8)	
G3	48 (20.6)	47 (20.2)	30 (12.9)	108 (46.4)	
Measurable Disease Before ChemoTherapy					***0.023***
No measurable disease	12 (8.3)	27 (18.8)	26 (18.1)	79 (54.9)	
Measurable disease	9 (15.3)	2 (3.4)	10 (16.9)	38 (64.4)	

Supplementary Table S8. BRCA1 and ovarian cancer

	BRCA1- N(%)	BRCA1+ N(%)	**P- value**
Pathological Type			**0.048**
Serous cystadenocarcinoma	62 (48.1)	67 (51.9)	
Mucinous cystadenocarcinoma	22 (66.7)	11 (33.3)	
Endometrioid	22 (75.9)	7 (24.1)	
Clear cell carcinoma	11 (57.9)	8 (42.1)	
Mixed	6 (54.5)	5 (45.5)	
FIGO Stage			**0.013**
I	63 (65.6)	33 (34.4)	
II	10 (33.3)	20 (66.7)	
III	48 (52.2)	44 (47.8)	
IV	2 (40.0)	3 (60.0)	
Tumour Grade			0.45
G1	19 (61.3)	12 (38.7)	
G2	25 (58.1)	18 (41.9)	
G3	62 (58.5)	61 (49.6)	
Measurable Disease pre-Chemotherapy			0.213
No measurable disease	88 (57.9)	64 (42.1)	
Measurable disease	27 (48.2)	29 (51.8)	

Supplementary Table S9: BRCA1/XRCC1 co-expression and Ovarian Cancer

	BRCA1-/ XRCC1- N(%)	**BRCA1-/ XRCC1+ N(%)**	**BRCA1+/ XRCC1 - N(%)**	**BRCA1+/ XRCC1 + N(%)**	**P- value**
Pathological Type					
Serous cystadenocarcinoma	16(12.8)	45(36.0)	3(2.4)	61(48.8)	
Mucinous cystadenocarcinoma	11(37.9)	9(31.0)	1(3.4)	8(27.6)	***0.029***
Endometrioid	6(22.2)	14(51.9)	0(0)	7(25.9)	
Clear cell carcinoma	7(38.9)	4(22.2)	0(0)	7(38.9)	
Mixed	0(0)	3(37.5)	1(12.5)	4(50)	
FIGO Stage					
I	27(30.3)	32(36.0)	1(1.1)	29(32.6)	
II	3(10.3)	6(20.7)	2(6.9)	18(62.1)	***0.024***
III	12(13.6)	35(39.8)	3(3.4)	38(43.2)	
IV	0(0)	2(40.0)	0(0)	3(60.0)	
Tumour Grade					
G1	9(33.3)	8(29.6)	1(3.7)	9(33.3)	*0.453*
G2	8(19)	17(40.5)	2(4.8)	15(35.7)	
G3	19(16.4)	40(34.5)	3(2.6)	54(46.6)	
Measurable Disease Before ChemoTherapy					
No measurable disease	34(24.3)	48(34.2)	2(1.4)	56(40.0)	***0.042***
Measurable disease	6(10.7)	21(37.5)	4(7.1)	25(44.6)	